

Learning Multimorbidity Patterns from Electronic Health Records Using Non-negative Matrix Factorisation

Abdelaali Hassaine · Dexter Canoy ·
Jose Roberto Ayala Solares · Yajie
Zhu · Shishir Rao · Yikuan Li · Kazem
Rahimi · Gholamreza Salimi-Khorshidi

18/07/2019

Abstract Multimorbidity, or the presence of several medical conditions in the same individual, have been increasing in the population both in absolute and relative terms. However, multimorbidity remains poorly understood, and the evidence from existing research to describe its burden, determinants and consequences have been limited. Many of these studies are often cross-sectional and do not explicitly account for multimorbidity patterns' evolution over time. Some studies were based on small datasets, used arbitrary or narrow age range, or lacked appropriate clinical validations. In this study, we applied Non-negative Matrix Factorisation (NMF) in a novel way to one of the largest electronic health records (EHR) databases in the world (with 4 million patients), for simultaneously modelling disease clusters and their role in one's multimorbidity over time. Furthermore, we demonstrated how the temporal characteristics that our model associates with each disease cluster can help mine disease trajectories/networks and generate new hypotheses for the formation of multimorbidity clusters as a function of time/ageing. Our results suggest that our method's ability to learn the underlying dynamics of diseases can provide the field with a novel data-driven / exploratory way of learning the patterns of multimorbidity and their interactions over time.

Keywords Non-negative Matrix Factorisation · Multimorbidity · Disease Trajectories · Electronic Health Records.

1 Introduction

Multimorbidity is generally defined as the presence of two or more chronic conditions in an individual [46]. There is growing evidence that the number

The George Institute for Global Health (UK), University of Oxford, United Kingdom
NIHR Oxford Biomedical Research Centre, Oxford University Hospitals NHS Foundation Trust, United Kingdom

of people with multimorbidity has been increasing in many populations, both in relative and absolute terms. This increasing burden has been attributed to a number of factors, including the trend towards an ageing population demographics, as well as factors relating to changes in lifestyle, health-seeking behaviour and the environment [44]. Research in this area has been growing, but most investigations have focused on predicting, preventing and managing disorders in isolation from one another. Therefore, more research is needed for a better understanding of this emerging burden, and its underlying patterns and mechanisms, in order to anticipate its consequences for the health services and the provision of appropriate care [32].

Different studies in the past have tried different methods to investigate the multimorbidity patterns (MMPs). The first group of such analyses are based on simple correlation/correspondence analyses, carried out on disease pairs; we refer to them as “pairwise methods”. For instance, Goldacre et al. [9] attempted to identify disease pairs, which show co-occurrence frequencies that are different from what their individual frequencies in the population would predict; disease pairs with higher or lower co-occurrences were interpreted as associated or dissociated, respectively. Hidalgo et al. [11] took pairwise methods further and built a disease network where the presence of an edge between two nodes (i.e., diseases) represented a strong correlations between them in the population they studied. They then showed the associations between the “connectedness” of the nodes and mortality. In a slightly different pairwise method that takes time into account, Jensen et al. [14] derived associations of disease pairs by taking into account the order in which they occur. They defined a concept called “disease trajectory clusters”, which can be viewed as a directed network, where each node represents a disease and an edge from disease A to B means that in many patients, B happened after A. Liu et al. [23] employed a slightly different pairwise method; they formed a network where nodes were medications, tests and diagnoses, and each edge’s weight and direction denoted an interval between the occurrence of the concepts and their order, respectively.

While pairwise methods are valuable in generating comorbidity hypotheses for disease pairs, their use to form large networks (and the use of resulting networks’ properties to draw medical conclusions) is likely to give misleading results. That is, when considering two diseases, there are other confounding diseases that are related to both diseases; this is known as the difference between correlation and partial correlation analysis [41]. This led to the rise of a second category of methods for the study of MMPs, which we refer to as “probabilistic methods”. In one of the earliest works in this category, Strauss et al. [42] used latent class growth analysis to identify clusters of multimorbidity trajectories but their analysis was based on a 3-year study period which is a relatively short time for the study of MMPs; furthermore, their study of temporal patterns was limited to counting chronic conditions recorded over time (rather than the study of how one disease’s occurrence is associated with other diseases’ occurrence). Wang et al. [50], on the other hand, used a Hidden Markov Model to study the generative process underlying the disease trajec-

tories. In their approach, the future relationship between latent comorbidity variables and observed diseases are determined by the current relationship between them over time. The key challenge of this approach is its high sensitivity to the current state of the model (rather than having a longer memory) and its computational complexity/expensiveness.

Another category of methods use deep learning to extract insights from EHRs. Many of these studies do not explicitly account for temporal information [45,25]. Nguyen et al. [27] introduced a CNN architecture called **Deepr** (Deep record), where a patient’s journey is modelled as a long sentence of medical codes where time between events are denoted as “special words”. The authors validated their method on hospital data to predict unplanned readmission after discharge. Another notable work is RETAIN (REverse Time Attention) model by Choi et al. [3] which used two RNNs and a two-level neural attention model to process sequential data using an end-to-end approach that has been tested on predicting heart failure diagnosis. Many recent works proposed similar architectures for different prediction tasks, including patients’ readmission [35,54], treatment recommendation [18] and personalized prescription [49]. Although deep learning methods usually minimise the need for pre-processing and feature engineering, the disease representations/associations they generate are biased toward the prediction task and are not necessarily generalisable to other tasks [53].

The other category of advanced methods that have been used to study multimorbidity, is primarily based on matrix/tensor decomposition and factor analysis; we refer to them as “factor methods”. In these methods, one usually starts by forming a matrix, where the entry i, j denotes a metric related to disease i (or other concepts in EHR, such as medication and/or clinical measurements) in patient j ; factor methods decompose such a matrix into P multimorbidity patterns. The resulting MMPs are described with two vectors: Disease clusters (that show the influence of each disease in that MMP), and the expression of that MMP in each patient. There have been multiple MMP analyses that used factor methods, but they did not take into account the temporal aspect of the diseases’ (co)occurrence and have been mostly limited to the study of disease clusters [13,39,24,17,38]. As one of the exceptions among factor methods, Zhou et al. [56] introduced a factor method that considers the temporal patterns in electronic health record (EHR) data; while the method has the potential to result in multimorbidity analyses, the study’s primary focus was on the prediction of future diseases. Given the non-negative nature of the data that such factor methods start from, non-negative factorisation techniques have also been used in this space. For instance, in both [12] and [51], non-negative tensor factorisation have been employed to learn the core factors underlying disease co-occurrences. If one represents the data to such tensor factorisation techniques in certain ways, these techniques have the ability to mine disease clusters and their temporal patterns. However, instead of time the focus was on joint patterns of phenotypes such as medication and diagnosis.

Table 1: The key papers dealing with the analysis of multimorbidity and disease trajectories

Paper (year)	Methodology	#patients	Handling of temporal trajectory	Age range
Goldacre et al. (2000) [9]	Rate of co-occurrence	2.5 million	For some diseases	All
Hidalgo et al. (2009) [11]	Network based on pairwise correlations	13 million	As a subsequent analysis	≥ 65
Wang et al. (2012) [48]	NMF	21K (all diabetic)	Up to one year	All
Jensen et al. (2014) [14]	Network based on pairwise correlations	6.2 million	5-year window	All
Strauss et al. (2014) [42]	Latent class growth modelling	24,615	Over 3 years	> 50
Wang et al. (2014) [50]	Hidden Markov Model	300,000	Over 4 years	All
Nguyen et al. (2017) [27]	Deep learning	300K	Through discretising	NA
Choi et al. (2016) [3]	Deep learning	263K	Yes	50 to 80 years
Rafiq et al. (2018) [35]	Deep learning	610	Yes	70 to 80 years
Xiao et al. (2018) [54]	Deep learning	Heart Failure cohort of 5,393 patients	Yes	NA
Le et al. (2018) [18]	Deep learning	6K and 5K	Yes	≥ 16
Ho et al. (2014) [12]	NMF	10,000	None	≥ 65
Zhou et al. (2014) [56]	QR factorisation	249 and 187	Up to 20 years	All
Wang et al. (2015) [51]	NMF	7,744 and 472,645	None	All
Liu et al. (2015) [23]	Decomposition of adjacency matrix of disease temporal graph	319,650	Over 4 years	All

In summary, various investigations have attempted to mine the MMPs from various sources of medical data - see Table 1. Most of these studies are limited to certain age ranges and/or are cross-sectional by design, which hampers their ability to observe the patients over an appropriate amount of time to see the temporal patterns of multimorbidity. Furthermore, in almost all these methods, time was not taken into account; a few of them that did account for progression over time, lacked appropriate MMP analysis and clinical validation (e.g., focused on disease prediction instead). For instance, in one of the most powerful factor methods (in terms of taking time into account), Wang et al. [48] used non-negative matrix factorisation (NMF), where each factor has a temporal evolution model; while this approach has the potential to provide unique insights into diseases trajectories and their interactions, it has only been validated on 21K patients with diabetes (i.e., limited data and clinical focus). Therefore, there is still need for an investigation of MMPs, using large datasets (that are representative of the population) and over a reasonable time horizon, which can simultaneously model disease clusters and their relationships/trajectories over time. The rapid growth in the development of healthcare information systems has led to an increased interest in utilising EHR. The longitudinal nature of EHR and its richness (e.g., containing diagnoses, medications, and tests/measurement) can provide a unique opportunity to study long-term patterns of diseases' cooccurrence.

In this study, we apply NMF [4,8] (with a novel design that results in both disease clusters and their trajectories) to one of the world's largest EHR datasets. Our approach (which falls in the factor method category) results in

two main characteristics for each MMP (or factor): a disease cluster (which like past factor methods is a vector showing the influences from each disease in that MMP) and the expression of that MMP in each patient at a given age. The expression of each MMP at a given age is the most important contribution of our paper; to demonstrate its importance, we carried out a follow-up analysis of building a multimorbidity network, where nodes are MMPs and an edge between two MMPs denotes their associations and/or likely influence on each other. The clinical validation of our results suggests that this new approach provides the field with a unique tool to study complex multimorbidity networks and their evolution as one ages.

2 Materials and methods

In this study, we are interested in understanding the MMPs, both in terms of disease clusters (i.e., disease co-occurrence patterns) and how they influence each other over time (i.e., their trajectories). In this section, we explain the source of our data, our use of NMF, and the follow-up analyses we carried out to show the strength of this approach as a foundation for future multimorbidity research. Note that, for the rest of the paper, matrices will be denoted by upper case bold fonts (e.g., **A**), vectors will be denoted by lower case bold fonts (e.g., **a**), and everything else (scalar and indices) will be denoted with no bolding of the fonts.

2.1 Data

In this study, we used CPRD (Clinical Practice Research Datalink) [5]; it contains longitudinal primary care data from a network of 674 general physician (GP) practices in the UK, and is linked to secondary care (i.e., Hospital Episode Statistics, or HES) and other health and administrative databases (e.g., office for national statistics' death registration). Around 1 in 10 GP practices in the UK contribute data to CPRD; it covers 35 million patients, among whom nearly 10 million are currently registered patients. CPRD is broadly representative of the population by age, sex, and ethnicity [10]. It has been extensively validated and is considered as the most comprehensive longitudinal primary care database [47], with several large-scale epidemiological reports [6, 7, 40] adding to its credibility.

HES, on the other hand, contains data on hospitalisations, outpatient visits, accident and emergency for all admissions to National Health Service (NHS) hospitals in England [21]. Approximately 75% of the CPRD GP practices in England (58% of all UK CPRD GP practices) participate in patient-level record linkage with HES, which is performed by the Health and Social Care Information Centre [26]. In this study, we only considered the data from GP practices that consented to (and hence have) record linkage with HES. The importance of primary care at the centre of the national health system in

Table 2: The number of diseases in each level of ICD-10 hierarchy

Level	Count	Example
ICD-10 chapter	22	II Neoplasms
ICD-10 sub-chapter	211	C00-C97 Malignant neoplasms
ICD-10 2 digits level	2049	C00 Malignant neoplasm of lip
ICD-10 full code	10138	C00.0 Malignant neoplasm: External upper lip

the UK, the additional linkages, and all the aforementioned properties, make CPRD one of the most suitable EHR datasets in the world for data-driven clinical/medical discovery and machine learning.

2.2 Study Population

In order to have a comprehensive coverage of patients’ health journey, we only considered the CPRD patients with at least 5 years of follow-up; this resulted in a total number of 2,204,178 patients with a total number of clinical 25,791,493 encounters. Note that, in this study, we are interested in “incident cases” and not in the “prevalent cases” of diseases, i.e. new occurrences of diseases rather than diseases carried over. Therefore, we only considered the first occurrence of each disease happening after 1 year of any patient’s registration date with the general practice clinic (as the first year after registration is likely to contain diseases carried over rather than new occurrences of diseases).

Another important step in processing CPRD was to create a consistent diseases classifications between GP and HES data and choosing the appropriate level of granularity in diseases’ hierarchy (see Table 2). In HES, diseases are coded using ICD-10 (International Classification of Diseases [52]) code, whereas in the GP records diseases are coded using Read Code [28]. ICD offers a hierarchical form that makes its use for data mining and machine learning much more convenient. Therefore, we decided to map the diseases to the ICD domain, i.e., we mapped the Read Codes to ICD-10 codes using the mapping provided by NHS Digital [29]. When no direct mapping was available, Read Codes were first mapped to SNOMED-CT codes [31] (also provided by NHS Digital [30]), and the latter are then mapped to ICD-10 codes using the mapping provided by the US National Library of Medicine [33].

As mentioned earlier, ICD-10 codes are organised in a tree-like hierarchy. Working at the highest level of the ICD-10 hierarchy will result in only a few diseases and hence is not likely to help unravel the complex underlying dependencies among diseases. Conversely, working at the lowest level of the hierarchy will generate thousands of diseases, each with small number of occurrences (and even a smaller number of co-occurrences) and hence an overall difficulty of mining useful inter-disease patterns. In this study, similarly to the work in [38], we chose to work at the ICD-10 sub-chapter level, which provides a good trade off between granularity and co-occurrence, and can lead to medically interpretable results. Furthermore, for the purpose of this study, we

eliminate all the diagnoses relating to pregnancy, general symptoms, external causes and administration (ICD-10 chapters XV, XVI, XVIII, XIX, XX and XXI); similar to [14]. The resulting 142 ICD-10 sub-chapters are what we will refer to as diseases from here on. the details of our inclusion/exclusion process is shown in Figure 1.

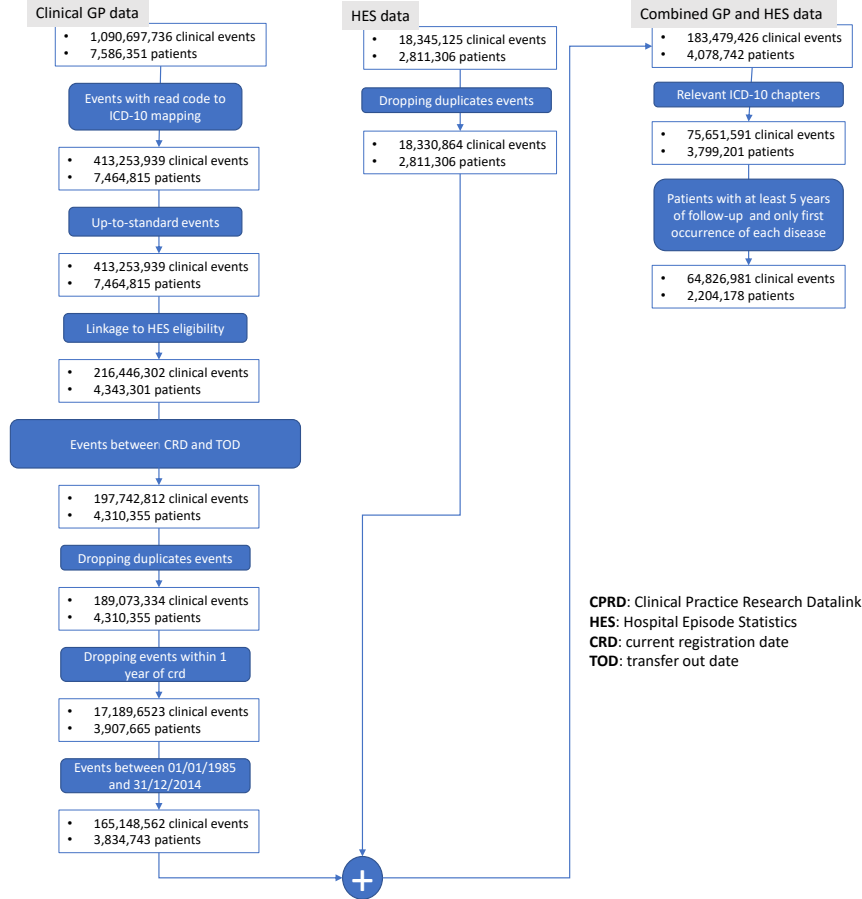


Fig. 1: Inclusion/exclusion criteria for the study. In order to make sure that the data is appropriate for the study’s objectives (described at the end of Section 1), we made sure that patients whose records meets our criteria (in terms of length, diseases, and quality of linkage) are only included. Also note that, terms such as “up to standard”, “crd” and “tod” are referring to fields in CPRD data; for more details on these, we refer readers to CPRD manual [5].

After all these, our cut of CPRD dataset includes nearly 2.2M adult patients (aged 16 years and over) and 65M events; from here, this will be referred to as the data in this study. Figure 2 shows some of the key characteristics of the data. When compared to the studies in Table 1, in terms of number of patients, length of follow-up and being representative of the population, our data is comparable, if not better, than the best ones studied so far.

2.3 Non-negative Matrix Factorisation

Non-negative matrix factorisation (NMF, or NNMF) refers to a group of algorithms that decompose a matrix \mathbf{D} into (usually) two matrices \mathbf{A} and \mathbf{B} , with the property that all three matrices have no negative elements, i.e.,

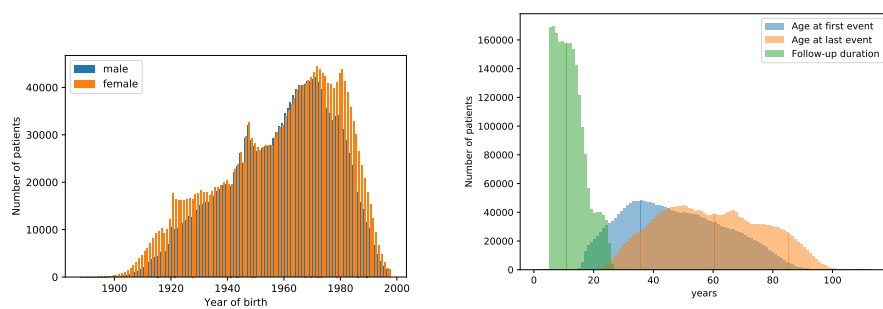
$$\mathbf{D} \approx \mathbf{A} \times \mathbf{B} \mid \mathbf{A} \geq 0, \mathbf{B} \geq 0. \quad (1)$$

This non-negativity makes the resulting matrices easier to inspect and interpret. Also, in applications such as processing of count data (i.e., the starting point of our multimorbidity analysis), non-negativity is inherent to the data being considered. Since the NMF problem does not have an exact analytical solution in general, there has been a range of numerical approximations for it [20, 22, 19, 15, 2, 55, 1, 57, 43, 16]. In this paper, we use the Kullback-Leibler divergence and simple multiplicative updates [20, 19], enhanced to avoid numerical underflow [2] as implemented by Nimfa python package [57]. Furthermore, in order to determine the number of factors (or, as in our analysis, the number of MMPs), we used the commonly applied cophenetic correlation coefficient, which measures the stability of clustering associated with a given rank [2].

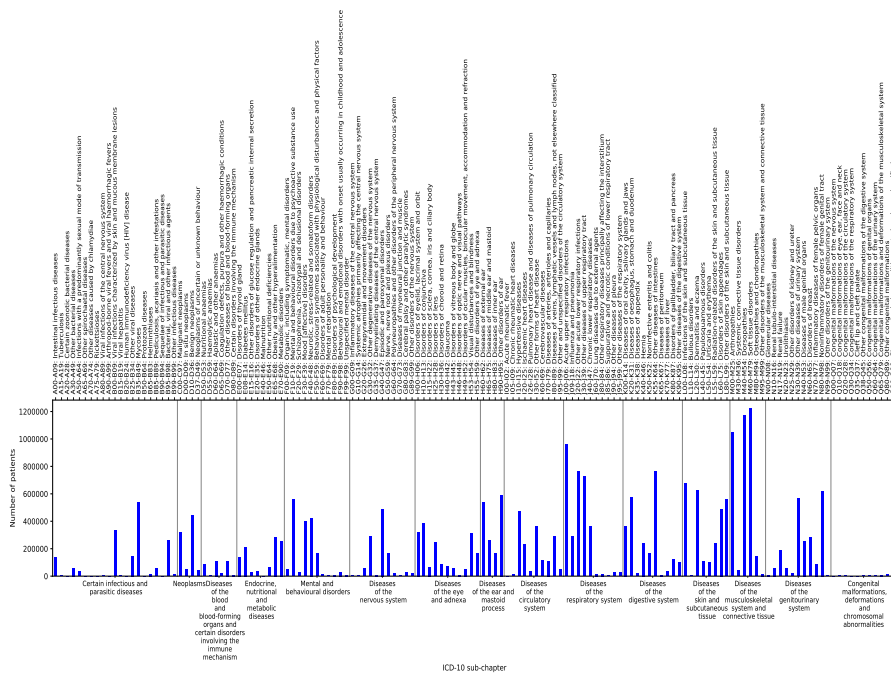
2.4 Modelling Pipeline

We start our modelling pipeline by forming a “disease matrix” \mathbf{D}_p for each patient p , where entry $d_{i,j}$ is 1 if patient p had the first incidence of disease i at age (in years) j ; $d_{i,j}$ will be 0 otherwise. This makes \mathbf{D}_p a $T \times C$ matrix, where C is the number of conditions/diseases (i.e., 142 in our case) and T is the maximum age we track a patient for (i.e., 114 years in our case). Denoting the total number patients by N , this process will result in N such \mathbf{D}_p matrices. We carry out two processing steps to create a final disease matrix \mathbf{D} for the NMF analysis.

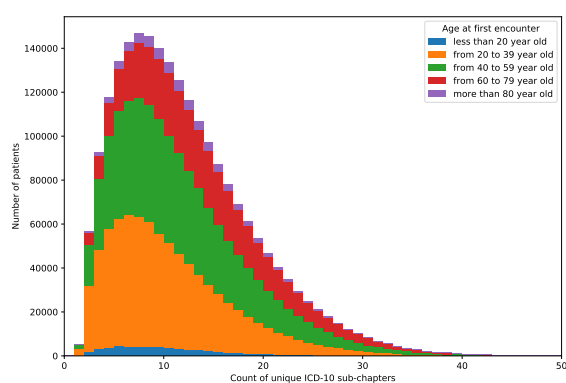
Given the variability in disease prevalences (i.e., some diseases are more common than others), the counts corresponding to rarer diseases (such as tuberculosis) are expected to be much lower than the counts corresponding to more common diseases such (such as respiratory infections). Therefore, when solving the NMF model, the results can be biased towards explaining the more frequent diseases/the higher counts. In order to correct for this, in our first processing step, we used an adjustment inspired by TF-IDF (term frequency-inverse document frequency) which is commonly used in natural



(a) Distribution of the patients' birth year (b) Distribution of patients' age at first and last visit, and follow-up duration



(c) Number of unique patients for each disease



(d) Number of patients for each disease, grouped by age ranges

Fig. 2: An exploratory analysis of the data.

language processing and information retrieval tasks [36]. More specifically, we introduce DF-IPF (disease frequency - inverse patient frequency), which equals $DF \times IPF$, where we set $DF = 1$ as we only considered the first occurrence of each disease. For each disease i , we then defined

$$IPF(i) = \log \frac{N}{\#\text{patients who had disease } i}, \quad (2)$$

where N is the total number of patients in our study. The DF-IPF adjustment for \mathbf{D}_p will simply result from the multiplication of its entries with the appropriate inverse patient frequency (i.e., $d_{i,j} \leftarrow d_{i,j} * IPF(i)$).

As each patient will only have a small subset of diseases, \mathbf{D}_p is expected to be sparse. On the other hand, NMF does not explicitly model age as a temporal concept with a covariance structure (i.e., no explicit model for the relationship among rows in \mathbf{D}). In medicine, however, one will not see a meaningful difference between a disease happening at age a or $a \pm \text{one or two years}$; they are virtually the same. In factorisation of a matrix like \mathbf{D} using standard NMF, however, this property will not exist and the two scenarios will not necessarily be seen as similar. Furthermore, we know from the practice of medicine that the date at which certain chronic disease gets recorded is a noisy concept, i.e., there is an inherent noise in the time of recording a diagnosis. For instance, a one's hypertension diagnosis can be delayed by months or years due to one ignoring the symptoms and/or delaying a doctor visit; or, diseases such dementia are known to have long preclinical periods, where patients who visit their doctors less regularly are on average more likely to have their diagnosis delayed.

Therefore, in a second adjustment of \mathbf{D}_p , and in order to tackle temporal forgetting of NMF and sparsity of the data, and take into account the noise/uncertainty we have around the age that a particular disease is recorded at, we smooth each column of \mathbf{D}_m , using a Gaussian filter with $\sigma = 3$ (in order to be able to learn patterns of diseases even when they are far apart). Figure 3 illustrates the effect of both these adjustments (DF-IPF and smoothing) on \mathbf{D}_p for an example patient.

Before we carry out the NMF analysis, we perform one last step: concatenating the \mathbf{D}_p matrices in age dimension to form \mathbf{D} (i.e., $\mathbf{D} = [\mathbf{D}_1, \mathbf{D}_2, \dots, \mathbf{D}_N]$); a $(T * N) \times C$ matrix. In other words, we assume that the relationship among diseases (i.e., the disease clusters) are in common among patients at all times, and it is their expression in different people at different ages that varies. Decomposing \mathbf{D} to Q MMPs, makes \mathbf{A} a $(T * N) \times Q$ matrix and \mathbf{B} a $Q \times C$ matrix. A row in \mathbf{B} will be an MMP's disease cluster, and a column in \mathbf{A} is an MMP's time course over patients during their life. See Figure 4 for an illustration of this process.

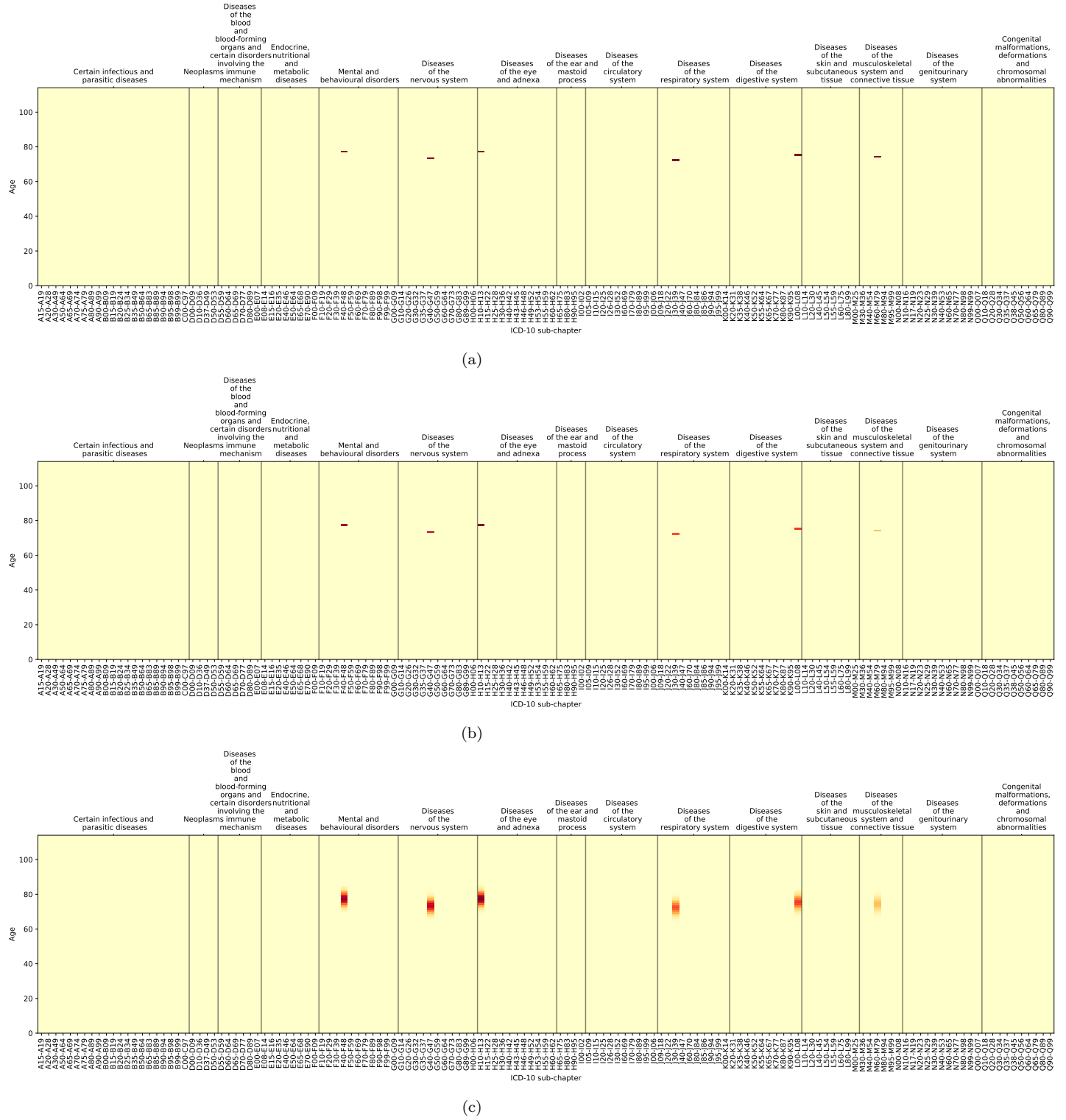


Fig. 3: The effect of adjustments on D_p . In (a), we show a sample D_p , where the patient had 6 diseases. The result of the DF-IPF adjustment is shown in (b), which can be seen visually as additional heat in the matrix, due to further strengthening of the cells that correspond to rare diseases. Lastly, when smoothed for each age year, as shown in (c), we see a less sparse D_p , where values of the nearby ages are similar for a given disease.

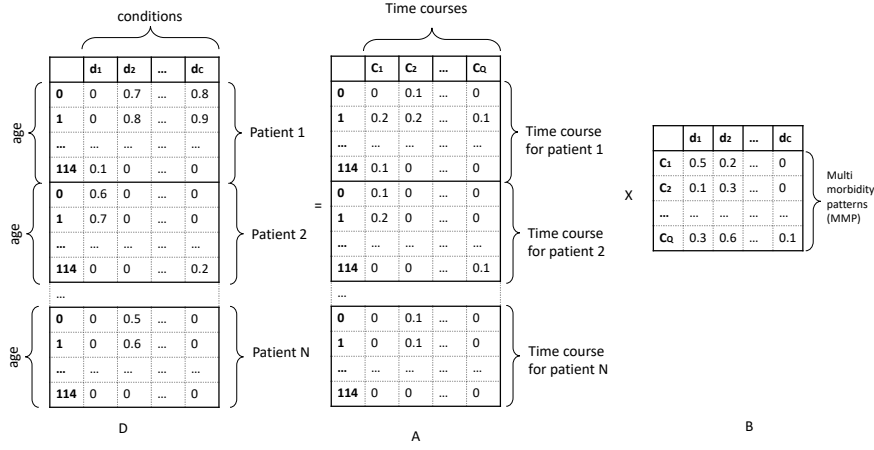


Fig. 4: An illustration of formation and decomposition of disease matrix **D**.

2.5 Ascendancy Analysis

One of the goals of multimorbidity analyses is to conclude how the presence of a disease or a disease cluster can increase the chance of another disease or disease cluster. This is essentially what network models do; a comprehensive study and review of a range of such techniques (for when the data from nodes/variables is available in the form of time-/event-course) can be found in Smith et al [41]. On the other hand, each MMP from our approach consists of a disease cluster and a pseudo time course (a patient-age course, to be more specific); for brevity we refer to the latter as time course. Therefore, in order to show the strength of our approach in providing the data for such follow-up studies of multimorbidity, we next employed a simple technique, which was introduced by Patel et al [34] for the study of the networks in the brain, for mining the network structure among MMPs. This idea is illustrated in Figure 5.

Imagine we have two MMPs, for which time courses \mathbf{v} and \mathbf{w} , are binary (say, via an appropriate thresholding applied to the continuous time course resulting from our NMF analysis). Now, if \mathbf{v} and \mathbf{w} are active together and inactive together, we consider them associated/connected. This concept is measured by $\kappa_{\mathbf{v},\mathbf{w}} \in [-1, 1]$, and can be seen as an undirected edge in a network; $\kappa_{\mathbf{v},\mathbf{w}}$ is 1 when the joint activation probability of \mathbf{v} and \mathbf{w} is the highest, -1 when the joint activation probability or the joint inactivation probability is nil, and 0 when \mathbf{v} and \mathbf{w} are statistically independent. Given the connectivity between \mathbf{v} and \mathbf{w} , if \mathbf{v} exhibits elevated activity for a subset of the period in which \mathbf{w} exhibits elevated activity, we consider \mathbf{w} to be ascendant to \mathbf{v} and vice versa. This is measured by $\tau_{\mathbf{v},\mathbf{w}} \in [-1, 1]$, and can be seen as a directional edge in a network; $\tau_{\mathbf{v},\mathbf{w}} > 0$ means that \mathbf{v} is ascendant to \mathbf{w} and $\tau_{\mathbf{v},\mathbf{w}} < 0$

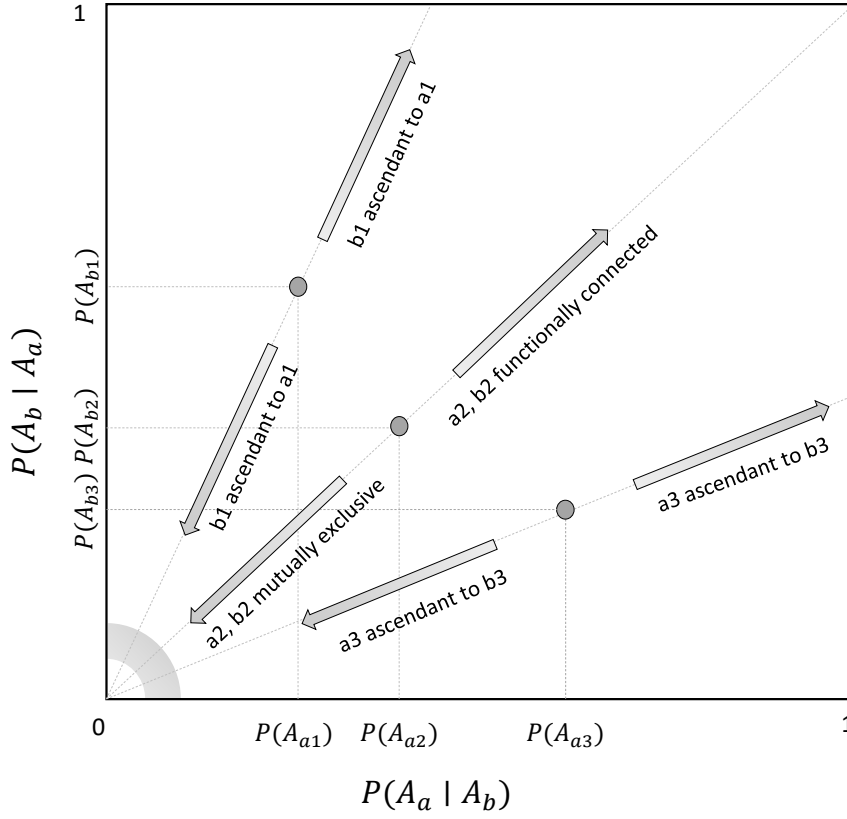


Fig. 5: Three MMP pairs (a_1, b_1) , (a_2, b_2) , and (a_3, b_3) are illustrated, each with a different hierarchical relationship. As the slope of the line from the origin to $(P(A_a), P(A_b))$ gets further from 1, the degree of ascendancy between the MMP pair increases. Credits to Patel et al. [34]

means that \mathbf{w} is ascendant to \mathbf{v} . We refer readers to the original paper for more details on the methods.

3 Results

As explained earlier, we first formed \mathbf{D} and used NMF to decompose it. Given that our implementation of NMF requires the number of factors to be given, we used cophenetic correlation coefficient to determine it; the result is shown in Figure 6. Based on the results we observed from a group of 100K randomly-selected patients, we chose the Q value of 34 as the optimal rank for the NMF.

Given that our approach does not explicitly model gender, we decided to carry out the analysis separately for men and women. In our data, we have

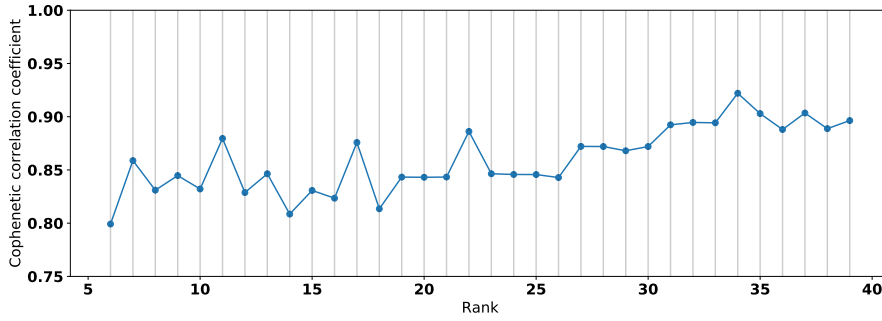


Fig. 6: The change in cophenetic coefficient (y axis) as a function of number of factors (x axis). As can be seen, 34 seems to be the optimal number for the number of factors that NMF will decompose \mathbf{D} into.

994,563 male and 1,209,615 female patients; Figure 7 shows the heatmap in which each column corresponds to disease clusters that result from NMF (i.e., matrix \mathbf{B}). Corresponding to each of these clusters we have a time course that has one value for every patient-age, which shows how a cluster has been expressed in that patient at that age (see Figure 8 for an example visualisation of this time series).

The components identified by our method are summarised in Table 3 for male patients and Table 4 for female patients. These tables give for each MMP, the top 3 diseases and their weights.

As discussed, while disease clusters are important, their trajectories over time (plus their influence on each other) is also important. One of the advantages of our approach is its ability to provide a time course for each disease clusters; treating each cluster as a node, this time course opens the door to a range of network modelling techniques that can help mine the patterns of interactions among the diseases. In this study, we used ascendancy analysis (described in Section 2.5) that was shown to be one of the most powerful techniques for mining directed and undirected edges in a network. Given that it requires the time courses to be binary, we binarised the time courses corresponding to each disease cluster by thresholding it at 5% of its maximum value (see Figure 8 for an illustration). Functional dependency and ascendancy between different MMPs, obtained through κ and τ , is illustrated in Figure 9.

If we only take the MMP pairs with high κ values, and define the direction of the edge between each pair using τ , a network can be achieved as shown in Figures 10 and 11. In these figures, we chose a threshold for κ , so that the obtained graph has 30 nodes; not too high to make interpretation difficult, and not too low to make the results less useful for clinical usability.

Table 3: Identified disease clusters for male patients.

1	J09-J18: Influenza and pneumonia (1.00) J90-J94: Other diseases of pleura (0.20) J20-J22: Other acute lower respiratory infections (0.18)	18	I60-I69: Cerebrovascular diseases (1.00) G40-G47: Episodic and paroxysmal disorders (0.43) G80-G83: Cerebral palsy and other paralytic syndromes (0.37)
2	N40-N53: Diseases of male genital organs (1.00) N30-N39: Other diseases of urinary system (0.17) A50-A64: Infections with a predominantly sexual mode of transmission (0.10)	19	H30-H36: Disorders of choroid and retina (1.00) H43-H45: Disorders of vitreous body and globe (0.49) H40-H42: Glaucoma (0.15)
3	H65-H75: Diseases of middle ear and mastoid (1.00) H90-H95: Other disorders of ear (0.50) J00-J06: Acute upper respiratory infections (0.14)	20	E08-E14: Diabetes mellitus (1.00) E15-E16: Other disorders of glucose regulation and pancreatic internal secretion (0.30) E65-E68: Obesity and other hyperalimentation (0.27)
4	A30-A49: Other bacterial diseases (1.00) J90-J94: Other diseases of pleura (0.21) E65-E68: Obesity and other hyperalimentation (0.16)	21	N20-N23: Urolithiasis (1.00) N10-N16: Renal tubulo-interstitial diseases (0.28) N30-N39: Other diseases of urinary system (0.15)
5	C00-C97: Malignant neoplasms (1.00) D37-D49: Neoplasms of uncertain or unknown behaviour (0.46) D00-D09: In situ neoplasms (0.31)	22	L40-L45: Papulosquamous disorders (1.00) E65-E68: Obesity and other hyperalimentation (0.65) F10-F19: Mental and behavioural disorders due to psychoactive substance use (0.19)
6	I80-I89: Diseases of veins, lymphatic vessels and lymph nodes, not elsewhere classified (1.00) I26-I28: Pulmonary heart disease and diseases of pulmonary circulation (0.19) L00-L08: Infections of the skin and subcutaneous tissue (0.14)	23	L55-L59: Radiation-related disorders of the skin and subcutaneous tissue (1.00) L80-L99: Other disorders of the skin and subcutaneous tissue (0.35) B00-B09: Viral infections characterized by skin and mucous membrane lesions (0.15)
7	D60-D64: Aplastic and other anaemias (1.00) D50-D53: Nutritional anaemias (0.91) D70-D77: Other diseases of blood and blood-forming organs (0.85)	24	E70-E90: Metabolic disorders (1.00) I10-I15: Hypertensive diseases (0.09) K70-K77: Diseases of liver (0.09)
8	F50-F59: Behavioural syndromes associated with physiological disturbances and physical factors (1.00) G40-G47: Episodic and paroxysmal disorders (0.07) M60-M79: Soft tissue disorders (0.07)	25	H53-H54: Visual disturbances and blindness (1.00) H15-H22: Disorders of sclera, cornea, iris and ciliary body (0.26) H55-H59: Other disorders of eye and adnexa (0.12)
9	N17-N19: Renal failure (1.00) I30-I52: Other forms of heart disease (0.85) I95-I99: Other and unspecified disorders of the circulatory system (0.46)	26	I10-I15: Hypertensive diseases (1.00) E65-E68: Obesity and other hyperalimentation (0.27) H80-H83: Diseases of inner ear (0.18)
10	K50-K52: Noninfective enteritis and colitis (1.00) K55-K64: Other diseases of intestines (0.17) L60-L75: Disorders of skin appendages (0.08)	27	K80-K87: Disorders of gallbladder, biliary tract and pancreas (1.00) K70-K77: Diseases of liver (0.40) K20-K31: Diseases of oesophagus, stomach and duodenum (0.17)
11	F30-F39: Mood [affective] disorders (1.00) G30-G32: Other degenerative diseases of the nervous system (0.96) F40-F48: Neurotic, stress-related and somatoform disorders (0.71)	28	H60-H62: Diseases of external ear (1.00) H90-H95: Other disorders of ear (0.40) G50-G59: Nerve, nerve root and plexus disorders (0.37)
12	I20-I25: Ischaemic heart diseases (1.00) I30-I52: Other forms of heart disease (0.23) J20-J22: Other acute lower respiratory infections (0.08)	29	F10-F19: Mental and behavioural disorders due to psychoactive substance use (1.00) K00-K14: Diseases of oral cavity, salivary glands and jaws (0.93) B95-B98: Bacterial, viral and other infectious agents (0.47)
13	B85-B89: Pediculosis, acariasis and other infestations (1.00) L20-L30: Dermatitis and eczema (0.20) L00-L08: Infections of the skin and subcutaneous tissue (0.15)	30	B25-B34: Other viral diseases (1.00) J00-J06: Acute upper respiratory infections (0.13) H80-H83: Diseases of inner ear (0.13)
14	D10-D36: Benign neoplasms (1.00) L80-L99: Other disorders of the skin and subcutaneous tissue (0.26) L60-L75: Disorders of skin appendages (0.18)	31	K90-K95: Other diseases of the digestive system (1.00) B00-B09: Viral infections characterized by skin and mucous membrane lesions (0.56) K20-K31: Diseases of oesophagus, stomach and duodenum (0.23)
15	K20-K31: Diseases of oesophagus, stomach and duodenum (1.00) J40-J47: Chronic lower respiratory diseases (0.94) J30-J39: Other diseases of upper respiratory tract (0.92)	32	H10-H13: Disorders of conjunctiva (1.00) H00-H06: Disorders of eyelid, lacrimal system and orbit (0.93) H55-H59: Other disorders of eye and adnexa (0.80)
16	K40-K46: Hernia (1.00) K20-K31: Diseases of oesophagus, stomach and duodenum (0.16) J40-J47: Chronic lower respiratory diseases (0.09)	33	H25-H28: Disorders of lens (1.00) H40-H42: Glaucoma (0.50) H15-H22: Disorders of sclera, cornea, iris and ciliary body (0.13)
17	A00-A09: Intestinal infectious diseases (1.00) G40-G47: Episodic and paroxysmal disorders (0.11) K55-K64: Other diseases of intestines (0.09)	34	I70-I79: Diseases of arteries, arterioles and capillaries (1.00) J40-J47: Chronic lower respiratory diseases (0.10) L80-L99: Other disorders of the skin and subcutaneous tissue (0.08)

Table 4: Identified disease clusters for female patients.

1	I30-I52: Other forms of heart disease (1.00) I20-I25: Ischaemic heart diseases (0.54) I60-I69: Cerebrovascular diseases (0.25)	18	E00-E07: Disorders of thyroid gland (1.00) I10-I15: Hypertensive diseases (0.12) E70-E90: Metabolic disorders (0.08)
2	A00-A09: Intestinal infectious diseases (1.00) G50-G59: Nerve, nerve root and plexus disorders (0.36) K20-K31: Diseases of oesophagus, stomach and duodenum (0.09)	19	G30-G32: Other degenerative diseases of the nervous system (1.00) F10-F19: Mental and behavioural disorders due to psychoactive substance use (0.24) F40-F48: Neurotic, stress-related and somatoform disorders (0.22)
3	H00-H06: Disorders of eyelid, lacrimal system and orbit (1.00) J40-J47: Chronic lower respiratory diseases (0.52) H10-H13: Disorders of conjunctiva (0.24)	20	I80-I89: Diseases of veins, lymphatic vessels and lymph nodes, not elsewhere classified (1.00) L00-L08: Infections of the skin and subcutaneous tissue (0.18) L80-L99: Other disorders of the skin and subcutaneous tissue (0.17)
4	H55-H59: Other disorders of eye and adnexa (1.00) H10-H13: Disorders of conjunctiva (0.32) H15-H22: Disorders of sclera, cornea, iris and ciliary body (0.21)	21	N80-N98: Noninflammatory disorders of female genital tract (1.00) D10-D36: Benign neoplasms (0.68) G50-G59: Nerve, nerve root and plexus disorders (0.41)
5	N60-N65: Disorders of breast (1.00) C00-C97: Malignant neoplasms (0.16) B35-B49: Mycoses (0.15)	22	M80-M94: Osteopathies and chondropathies (1.00) M30-M36: Systemic connective tissue disorders (0.12) K20-K31: Diseases of oesophagus, stomach and duodenum (0.12)
6	K00-K14: Diseases of oral cavity, salivary glands and jaws (1.00) H10-H13: Disorders of conjunctiva (0.59) H53-H54: Visual disturbances and blindness (0.24)	23	E20-E35: Disorders of other endocrine glands (1.00) H15-H22: Disorders of sclera, cornea, iris and ciliary body (0.72) L40-L45: Papulosquamous disorders (0.18)
7	J09-J18: Influenza and pneumonia (1.00) J20-J22: Other acute lower respiratory infections (0.17) G40-G47: Episodic and paroxysmal disorders (0.16)	24	H65-H75: Diseases of middle ear and mastoid (1.00) H90-H95: Other disorders of ear (0.39) H60-H62: Diseases of external ear (0.31)
8	H80-H83: Diseases of inner ear (1.00) H90-H95: Other disorders of ear (0.16) H60-H62: Diseases of external ear (0.10)	25	B85-B89: Pediculosis, acariasis and other infestations (1.00) B35-B49: Mycoses (0.26) L20-L30: Dermatitis and eczema (0.22)
9	N30-N39: Other diseases of urinary system (1.00) E70-E90: Metabolic disorders (0.47) J20-J22: Other acute lower respiratory infections (0.38)	26	E50-E64: Other nutritional deficiencies (1.00) D50-D53: Nutritional anaemias (0.21) L55-L59: Radiation-related disorders of the skin and subcutaneous tissue (0.11)
10	D60-D64: Aplastic and other anaemias (1.00) D50-D53: Nutritional anaemias (0.66) K90-K95: Other diseases of the digestive system (0.35)	27	K80-K87: Disorders of gallbladder, biliary tract and pancreas (1.00) K20-K31: Diseases of oesophagus, stomach and duodenum (0.30) K40-K46: Hernia (0.26)
11	K50-K52: Noninfective enteritis and colitis (1.00) K55-K64: Other diseases of intestines (0.16) K90-K95: Other diseases of the digestive system (0.14)	28	N17-N19: Renal failure (1.00) I10-I15: Hypertensive diseases (0.39) E08-E14: Diabetes mellitus (0.37)
12	H25-H28: Disorders of lens (1.00) H53-H54: Visual disturbances and blindness (0.89) H30-H36: Disorders of choroid and retina (0.69)	29	I70-I79: Diseases of arteries, arterioles and capillaries (1.00) M30-M36: Systemic connective tissue disorders (0.36) L40-L45: Papulosquamous disorders (0.20)
13	F30-F39: Mood [affective] disorders (1.00) F40-F48: Neurotic, stress-related and somatoform disorders (0.68) G40-G47: Episodic and paroxysmal disorders (0.45)	30	D70-D77: Other diseases of blood and blood-forming organs (1.00) D50-D53: Nutritional anaemias (0.24) K20-K31: Diseases of oesophagus, stomach and duodenum (0.10)
14	E65-E68: Obesity and other hyperalimentation (1.00) E08-E14: Diabetes mellitus (0.41) I10-I15: Hypertensive diseases (0.21)	31	B00-B09: Viral infections characterized by skin and mucous membrane lesions (1.00) L55-L59: Radiation-related disorders of the skin and subcutaneous tissue (0.29) K20-K31: Diseases of oesophagus, stomach and duodenum (0.19)
15	N10-N16: Renal tubulo-interstitial diseases (1.00) N20-N23: Urolithiasis (0.25) N30-N39: Other diseases of urinary system (0.12)	32	H49-H52: Disorders of ocular muscles, binocular movement, accommodation and refraction (1.00) C00-C97: Malignant neoplasms (0.32) G20-G26: Extrapyrimal and movement disorders (0.20)
16	L50-L54: Urticaria and erythema (1.00) L20-L30: Dermatitis and eczema (0.18) L60-L75: Disorders of skin appendages (0.15)	33	N70-N77: Inflammatory diseases of female pelvic organs (1.00) B35-B49: Mycoses (0.17) N80-N98: Noninflammatory disorders of female genital tract (0.17)
17	B95-B98: Bacterial, viral and other infectious agents (1.00) J30-J39: Other diseases of upper respiratory tract (0.23) B35-B49: Mycoses (0.21)	34	B25-B34: Other viral diseases (1.00) H60-H62: Diseases of external ear (0.35) J30-J39: Other diseases of upper respiratory tract (0.33)

4 Conclusions and Discussion

In this study, we employed a well-known matrix factorisation technique (i.e., NMF) to mine the MMPs from one of the largest EHR datasets in the world (i.e., CPRD). The key reason behind this research was to provide a solution for the shortcomings of the state-of-the-art data-driven multimorbidity research. To be more specific, our study attempted to build on the past studies' learnings, while minimising risks such as using relatively small data, relying on a narrow observation window, focusing on a small number of diseases, and solely extracting the disease clusters (instead of also extracting their trajectories and how they interact with each other over time).

Our approach is exploratory (or, data-driven) and hence the results will require thorough clinical validation. Therefore, in a follow-up analysis, we compared the MMPs resulting from our analysis with multimorbidity patterns published by other studies that went through thorough clinical validations; more specifically, we considered the study by Jensen et al. for which the list of directional ICD-10 diagnosis pairs are provided [14]. For the comparison to hold, for each ICD-10 code we generated the corresponding ICD-10 sub-chapter. After excluding pairs where the two ICD-10 sub-chapters are the same, this results in 1,556 unique ICD-10 sub-chapter pairs. Next, for each MMP we considered the top 10 diseases. Out of 1,556 ICD-10 sub-chapter pairs by Jensen et al., 411 pairs (26.4%) belong to the top 10 diseases of at least one of the 34 obtained MMPs of male patients, that is 1.879 higher (95% CI 1.866-1.892) than what would be obtained through random sampling. Similarly, 430 pairs (27.6%) belong to the top 10 diseases of at least one of the 34 obtained MMPs of female patients, which is 1.969 higher (95% CI 1.956-1.983) than what would be obtained through random sampling. When considering the top 3 diseases, the overlap will be 3.861 higher than random sampling (95% CI 3.783-3.939) for male patients and 3.962 (95% CI 3.880-4.045) for female patients.

Furthermore, to clinically validate our ascendancy results, we have computed the number of pairs by Jensen et al. that traverse our ascendancy graphs when choosing κ in a similar way to figures 10 and 11 and when considering the top 10 diseases for each MMP. These were 328 for male patients, which is higher than random sampling by a factor of 1.629 (95% CI 1.615-1.644) and 320 for female patients, which is higher than random sampling by a factor of 1.431 (95% CI 1.420-1.443). When considering the top 3 diseases, those number become 45 for male patients, higher than random sampling by a factor of 2.468 (95% CI 2.411-2.526) and 48 for female patients, higher than random sampling by a factor of 2.277 (95% CI 2.230-2.325). All these validate the fact that our approach, despite being purely data-driven, shows strong correspondence to some of the reliable MMP studies that have been clinically validated. Despite this, we believe that the field will benefit from future research into a more thorough clinical investigation of the results from the approach we introduced.

An important objective of multimorbidity analyses is to conclude a disease network, which summarises how diseases interact with one another and influence each other’s trajectories. While network models have the potential to solve such a problem, if given the time courses for diseases, the definition of nodes can be a challenge for researchers. As Table 2 shows, if we operate in the ICD-10 universe, we can see scenarios where the network can have anything ranging from 22 nodes to 10,138 nodes; prior to starting the network analysis, one needs to make this decision that at what level of this hierarchy will they define the diseases and hence nodes. We know from the network modelling literature that the search space for finding the best network is of a super-exponential size on the number of nodes (i.e., $O(n!2^{\binom{n}{2}})$) [37]. This makes the optimisation for learning a network of 10K nodes a huge challenge; both in terms of data (relatively small number of patients, and low prevalence and hence cooccurrence of most diseases at this level) and computing. On the other hand, using ICD-10 chapters, which will result in network with 22 nodes, is likely to lead to results that are hard to be clinically meaningful/interpretable; due to the heterogeneity of the diseases they each contain. Operating at levels such as sub-chapters and 2-digit ICD-10 codes is likely to have many highly correlated/co-occurring nodes that might make sense to be combined (particularly, given the data and computing challenges that we face when learning large networks).

Therefore, in this study, we introduced a new concept for the node: the disease clusters resulting from the NMF. This definition of nodes has a few advantages. Firstly, as our analysis suggests, it leads to a relatively small number of nodes, for which the corresponding network will be easier to learn. Secondly, from an empirical point of view, given that such nodes are driven by diseases that usually cooccur, splitting them into sub-nodes is not likely to be the source of any advantage (specially that such a split will make the network more complex and hence more difficult to learn). And lastly, from a clinical way of thinking, we are implying that diseases tend to happen in clusters and what the network will tell us is the influence of one cluster on another, given the rest of the clusters. This is in correspondence with what many in the clinical world have been arguing for that the definition of diseases today might not be the most accurate one (and hence various research on phenomapping of the diseases). Based on all these, we carried out our analysis and derived a network, using a simple and yet powerful technique known as ascendancy analysis. Of course, the data from our NMF approach is equally useful for any other network model (e.g., Bayesian networks), and hence there is need for follow-up research on the use of alternative network modelling techniques (an exhaustive list of such techniques have been used and compared in Smith et al [41]).

As in most such analyses, our modelling pipeline relied on a mix of choices we made; from preprocessing to factorisation technique and beyond. For instance, NMF has a range of different implementations; a follow-up research on comparing different implementations of NMF can surely improve the ap-

proach we introduced. Furthermore, the data preprocessing we introduced, from smoothing to adjustment for count can all be done with some differences that can be subject of future research. Lastly, our approach was focused on **D** as defined in Section 2. The earlier works, however, have introduced more concepts (e.g., measurements and medications) to the starting matrix, and some even went further and introduced a tensor as their starting point. A combination of our approach and such works can lead to richer multimorbidity analyses that not only can take time/age into account, but also can benefit from additional concepts and interventions that do influence the disease clusters and their trajectories.

Acknowledgements This research was funded by the Oxford Martin School (OMS) and supported by the National Institute for Health Research (NIHR) Oxford Biomedical Research Centre (BRC). The views expressed are those of the authors and not necessarily those of the OMS, the UK National Health Service (NHS), the NIHR or the Department of Health and Social Care. This work uses data provided by patients and collected by the NHS as part of their care and support and would not have been possible without access to this data. The NIHR recognises and values the role of patient data, securely accessed and stored, both in underpinning and leading to improvements in research and care.

References

1. Morten Arngren, Mikkel N Schmidt, and Jan Larsen. Bayesian nonnegative matrix factorization with volume prior for unmixing of hyperspectral images. In *2009 IEEE International Workshop on Machine Learning for Signal Processing*, pages 1–6. IEEE, 2009.
2. Jean-Philippe Brunet, Pablo Tamayo, Todd R Golub, and Jill P Mesirov. Metagenes and molecular pattern discovery using matrix factorization. *Proceedings of the national academy of sciences*, 101(12):4164–4169, 2004.
3. Edward Choi, Mohammad Taha Bahadori, Jimeng Sun, Joshua Kulas, Andy Schuetz, and Walter Stewart. Retain: An interpretable predictive model for healthcare using reverse time attention mechanism. In *Advances in Neural Information Processing Systems*, pages 3504–3512, 2016.
4. Andrzej Cichocki and Anh-Huy Phan. Fast local algorithms for large scale nonnegative matrix and tensor factorizations. *IEICE transactions on fundamentals of electronics, communications and computer sciences*, 92(3):708–721, 2009.
5. Clinical practice research datalink. available at: <https://www.cprd.com/>.
6. Connor A Emdin, Simon G Anderson, Thomas Callender, Nathalie Conrad, Gholamreza Salimi-Khorshidi, Hamid Mohseni, Mark Woodward, and Kazem Rahimi. Usual blood pressure, peripheral arterial disease, and vascular risk: cohort study of 4.2 million adults. *Bmj*, 351:h4865, 2015.
7. Connor A Emdin, Simon G Anderson, Gholamreza Salimi-Khorshidi, Mark Woodward, Stephen MacMahon, Terrence Dwyer, and Kazem Rahimi. Usual blood pressure, atrial fibrillation and vascular risk: evidence from 4.3 million adults. *International journal of epidemiology*, 46(1):162–172, 2016.
8. Cédric Févotte and Jérôme Idier. Algorithms for nonnegative matrix factorization with the β -divergence. *Neural computation*, 23(9):2421–2456, 2011.
9. M Goldacre, L Kurina, D Yeates, V Seagroatt, and L Gill. Use of large medical databases to study associations between diseases. *Qjm*, 93(10):669–675, 2000.
10. Emily Herrett, Arlene M Gallagher, Krishnan Bhaskaran, Harriet Forbes, Rohini Mathur, Tjeerd van Staa, and Liam Smeeth. Data resource profile: clinical practice research datalink (cprd). *International journal of epidemiology*, 44(3):827–836, 2015.

11. César A Hidalgo, Nicholas Blumm, Albert-László Barabási, and Nicholas A Christakis. A dynamic network approach for the study of human phenotypes. *PLoS computational biology*, 5(4):e1000353, 2009.
12. Joyce C Ho, Joydeep Ghosh, and Jimeng Sun. Marble: high-throughput phenotyping from electronic health records via sparse nonnegative tensor factorization. In *Proceedings of the 20th ACM SIGKDD international conference on Knowledge discovery and data mining*, pages 115–124. ACM, 2014.
13. Libby Holden, Paul A Scuffham, Michael F Hilton, Alexander Muspratt, Shu-Kay Ng, and Harvey A Whiteford. Patterns of multimorbidity in working australians. *Population health metrics*, 9(1):15, 2011.
14. Anders Boeck Jensen, Pope L Moseley, Tudor I Oprea, Sabrina Gade Ellesøe, Robert Eriksson, Henriette Schmock, Peter Bjødstrup Jensen, Lars Juhl Jensen, and Søren Brunak. Temporal disease trajectories condensed from population-wide registry data covering 6.2 million patients. *Nature communications*, 5:4022, 2014.
15. Yuan Wang Yunde Jia and Changbo Hu Matthew Turk. Fisher non-negative matrix factorization for learning local features. In *Proc. Asian conf. on comp. vision*, pages 27–30. Citeseer, 2004.
16. Michael Kapralov, Vamsi Potluru, and David Woodruff. How to fake multiply by a gaussian matrix. In *International Conference on Machine Learning*, pages 2101–2110, 2016.
17. Inge Kirchberger, Christa Meisinger, Margit Heier, Anja-Kerstin Zimmermann, Barbara Thorand, Christine S Autenrieth, Annette Peters, Karl-Heinz Ladwig, and Angela Döring. Patterns of multimorbidity in the aged population. results from the kora-age study. *PloS one*, 7(1):e30556, 2012.
18. Hung Le, Truyen Tran, and Svetha Venkatesh. Dual control memory augmented neural networks for treatment recommendations. In *Pacific-Asia Conference on Knowledge Discovery and Data Mining*, pages 273–284. Springer, 2018.
19. Daniel D Lee and H Sebastian Seung. Learning the parts of objects by non-negative matrix factorization. *Nature*, 401(6755):788, 1999.
20. Daniel D Lee and H Sebastian Seung. Algorithms for non-negative matrix factorization. In *Advances in neural information processing systems*, pages 556–562, 2001.
21. F Lee, HRH Patel, and M Emberton. The top 10urological procedures: a study of hospital episodes statistics 1998–99. *BJU international*, 90(1):1–6, 2002.
22. Stan Z Li, XinWen Hou, HongJiang Zhang, and QianSheng Cheng. Learning spatially localized, parts-based representation. *CVPR (1)*, 207:212, 2001.
23. Chuanren Liu, Fei Wang, Jianying Hu, and Hui Xiong. Temporal phenotyping from longitudinal electronic health records: A graph based framework. In *Proceedings of the 21th ACM SIGKDD international conference on knowledge discovery and data mining*, pages 705–714. ACM, 2015.
24. Alessandra Marengoni, Debora Rizzuto, Hui-Xin Wang, Bengt Winblad, and Laura Fratiglioni. Patterns of chronic multimorbidity in the elderly population. *Journal of the American Geriatrics Society*, 57(2):225–230, 2009.
25. Riccardo Miotto, Li Li, Brian A Kidd, and Joel T Dudley. Deep patient: an unsupervised representation to predict the future of patients from the electronic health records. *Scientific reports*, 6:26094, 2016.
26. Hamid Mohseni, Amit Kiran, Reza Khorshidi, and Kazem Rahimi. Influenza vaccination and risk of hospitalization in patients with heart failure: a self-controlled case series study. *European heart journal*, 38(5):326–333, 2017.
27. P. Nguyen, T. Tran, N. Wickramasinghe, and S. Venkatesh. Deepr: A convolutional net for medical records. *IEEE Journal of Biomedical and Health Informatics*, 21(1):22–30, Jan 2017.
28. NHS-Digital. Read codes. Available at: <https://digital.nhs.uk/services/terminology-and-classifications/read-codes>.
29. NHS-Digital. Read-ICD10 cross map. <https://nhs-digital.citizenspace.com/uktc/crossmaps/>.
30. NHS-Digital. Read v2 to SNOMED CT Mapping Lookup (October 2018). https://hscic.kahootz.com/connect.ti/t_c_home/view?objectId=407588.
31. NHS-Digital. Snomed codes. <https://digital.nhs.uk/services/terminology-and-classifications/snomed-ct>.

32. The Academy of Medical Sciences. Multimorbidity: a priority for global health research, 2018. <https://acmedsci.ac.uk/policy/policy-projects/multimorbidity>.
33. National Library of Medicine. Snomed ct to icd-10-cm map. https://www.nlm.nih.gov/research/umls/mapping_projects/snomedct_to_icd10cm.html.
34. Rajan S Patel, F DuBois Bowman, and James K Rilling. A bayesian approach to determining connectivity of the human brain. *Human brain mapping*, 27(3):267–276, 2006.
35. Muhammad Rafiq, George Keel, Pamela Mazzocato, Jonas Spaak, Carl Savage, and Christian Guttman. Deep learning architectures for vector representations of patients and exploring predictors of 30-day hospital readmissions in patients with multiple chronic conditions. In *International Workshop on Artificial Intelligence in Health*, pages 228–244. Springer, 2018.
36. Anand Rajaraman and Jeffrey David Ullman. *Mining of massive datasets*. Cambridge University Press, 2011.
37. Robert W Robinson. Counting labeled acyclic digraphs, new directions in the theory of graphs (proc. third ann arbor conf., univ. michigan, ann arbor, mich., 1971), 1973.
38. Albert Roso-Llorach, Concepción Violán, Quintí Foguet-Boreu, Teresa Rodríguez-Blanco, Mariona Pons-Vigués, Enriqueta Pujol-Ribera, and Jose Maria Valderas. Comparative analysis of methods for identifying multimorbidity patterns: a study of real-world data. *BMJ open*, 8(3):e018986, 2018.
39. Ingmar Schäfer, Eike-Christin von Leitner, Gerhard Schön, Daniela Koller, Heike Hansen, Tina Kolonko, Hanna Kaduszkiewicz, Karl Wegscheider, Gerd Glaeske, and Hendrik van den Bussche. Multimorbidity patterns in the elderly: a new approach of disease clustering identifies complex interrelations between chronic conditions. *PloS one*, 5(12):e15941, 2010.
40. Liam Smeeth, Sara L Thomas, Andrew J Hall, Richard Hubbard, Paddy Farrington, and Patrick Vallance. Risk of myocardial infarction and stroke after acute infection or vaccination. *New England Journal of Medicine*, 351(25):2611–2618, 2004.
41. Stephen M Smith, Karla L Miller, Gholamreza Salimi-Khorshidi, Matthew Webster, Christian F Beckmann, Thomas E Nichols, Joseph D Ramsey, and Mark W Woolrich. Network modelling methods for fmri. *Neuroimage*, 54(2):875–891, 2011.
42. Vicky Y Strauss, Peter W Jones, Umesh T Kadam, and Kelvin P Jordan. Distinct trajectories of multimorbidity in primary care were identified using latent class growth analysis. *Journal of clinical epidemiology*, 67(10):1163–1171, 2014.
43. Mariano Tepper and Guillermo Sapiro. Compressed nonnegative matrix factorization is fast and accurate. *IEEE Transactions on Signal Processing*, 64(9):2269–2283, 2016.
44. Jenny Tran, Robyn Norton, Nathalie Conrad, Fatemeh Rahimian, Dexter Canoy, Milad Nazarzadeh, and Kazem Rahimi. Patterns and temporal trends of comorbidity among adult patients with incident cardiovascular disease in the uk between 2000 and 2014: A population-based cohort study. *PLoS medicine*, 15(3):e1002513, 2018.
45. Truyen Tran, Tu Dinh Nguyen, Dinh Phung, and Svetha Venkatesh. Learning vector representation of medical objects via emr-driven nonnegative restricted boltzmann machines (enrbm). *Journal of biomedical informatics*, 54:96–105, 2015.
46. Marjan Van den Akker, Frank Buntinx, Job FM Metsemakers, Sjeef Roos, and J André Knottnerus. Multimorbidity in general practice: prevalence, incidence, and determinants of co-occurring chronic and recurrent diseases. *Journal of clinical epidemiology*, 51(5):367–375, 1998.
47. T Walley and A Mantgani. The uk general practice research database. *The Lancet*, 350(9084):1097–1099, 1997.
48. Fei Wang, Noah Lee, Jianying Hu, Jimeng Sun, and Shahram Ebadollahi. Towards heterogeneous temporal clinical event pattern discovery: a convolutional approach. In *Proceedings of the 18th ACM SIGKDD international conference on Knowledge discovery and data mining*, pages 453–461. ACM, 2012.
49. Lu Wang, Wei Zhang, Xiaofeng He, and Hongyuan Zha. Personalized prescription for comorbidity. In *International Conference on Database Systems for Advanced Applications*, pages 3–19. Springer, 2018.
50. Xiang Wang, David Sontag, and Fei Wang. Unsupervised learning of disease progression models. In *Proceedings of the 20th ACM SIGKDD international conference on Knowledge discovery and data mining*, pages 85–94. ACM, 2014.

51. Yichen Wang, Robert Chen, Joydeep Ghosh, Joshua C Denny, Abel Kho, You Chen, Bradley A Malin, and Jimeng Sun. Rubik: Knowledge guided tensor factorization and completion for health data analytics. In *Proceedings of the 21th ACM SIGKDD International Conference on Knowledge Discovery and Data Mining*, pages 1265–1274. ACM, 2015.
52. WHO International Classification of Diseases, ICD-10 version 2016. available at: <https://icd.who.int/browse10/2016/en>.
53. Cao Xiao, Edward Choi, and Jimeng Sun. Opportunities and challenges in developing deep learning models using electronic health records data: a systematic review. *Journal of the American Medical Informatics Association*, 25(10):1419–1428, 2018.
54. Cao Xiao, Tengfei Ma, Adji B Dieng, David M Blei, and Fei Wang. Readmission prediction via deep contextual embedding of clinical concepts. *PloS one*, 13(4):e0195024, 2018.
55. Zhongyuan Zhang, Tao Li, Chris Ding, and Xiangsun Zhang. Binary matrix factorization with applications. In *Seventh IEEE International Conference on Data Mining (ICDM 2007)*, pages 391–400. IEEE, 2007.
56. Jiayu Zhou, Fei Wang, Jianying Hu, and Jieping Ye. From micro to macro: data driven phenotyping by densification of longitudinal electronic medical records. In *Proceedings of the 20th ACM SIGKDD international conference on Knowledge discovery and data mining*, pages 135–144. ACM, 2014.
57. Marinka Zitnik and Blaz Zupan. Nimfa: A python library for nonnegative matrix factorization. *Journal of Machine Learning Research*, 13:849–853, 2012.

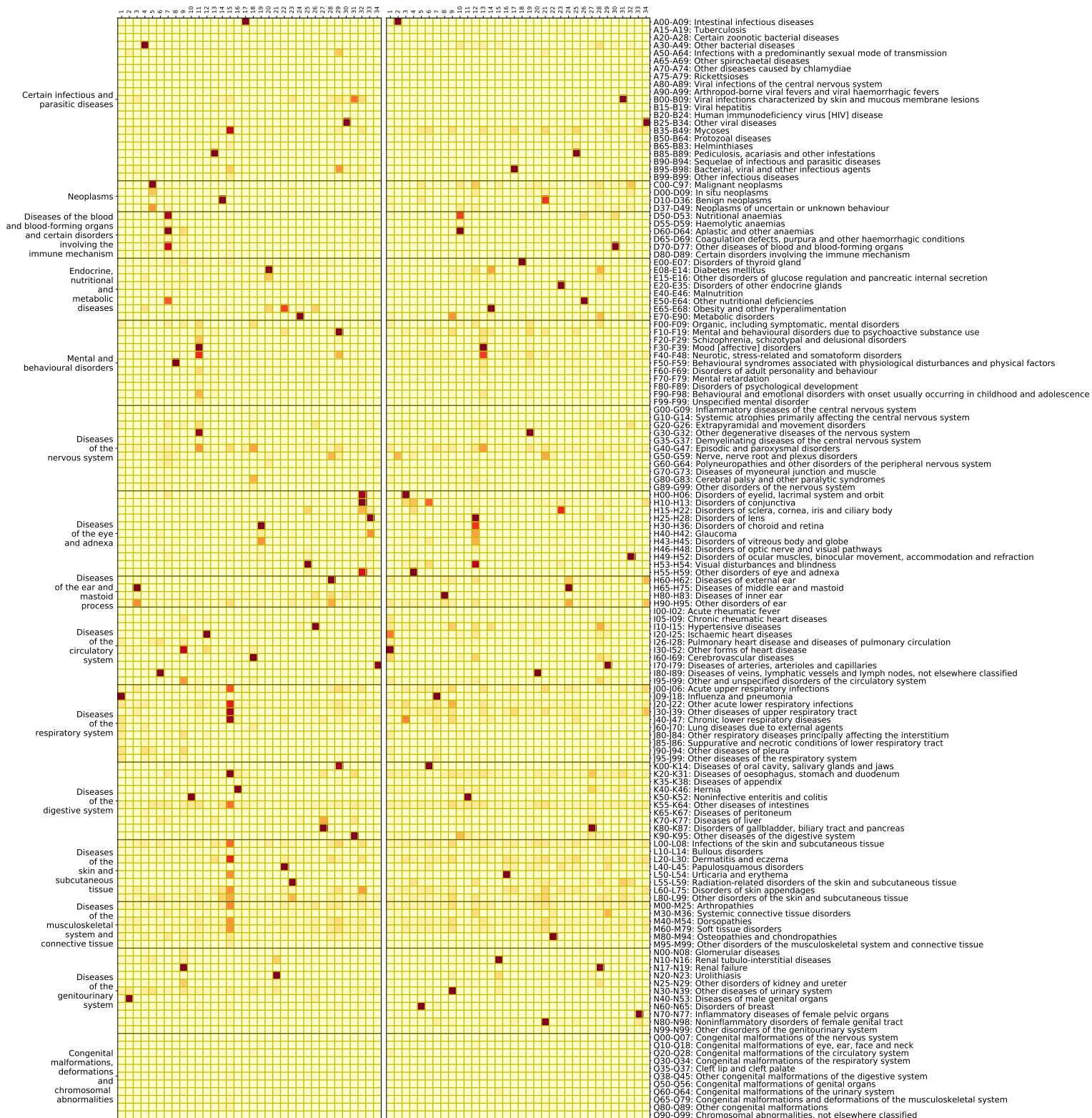


Fig. 7: Multi-morbidity components of male patients on the left side and female patients on the right side (gamma correction is applied so that small values are visible). Note that we show a transposed version (B^T) of B matrices for clarity.

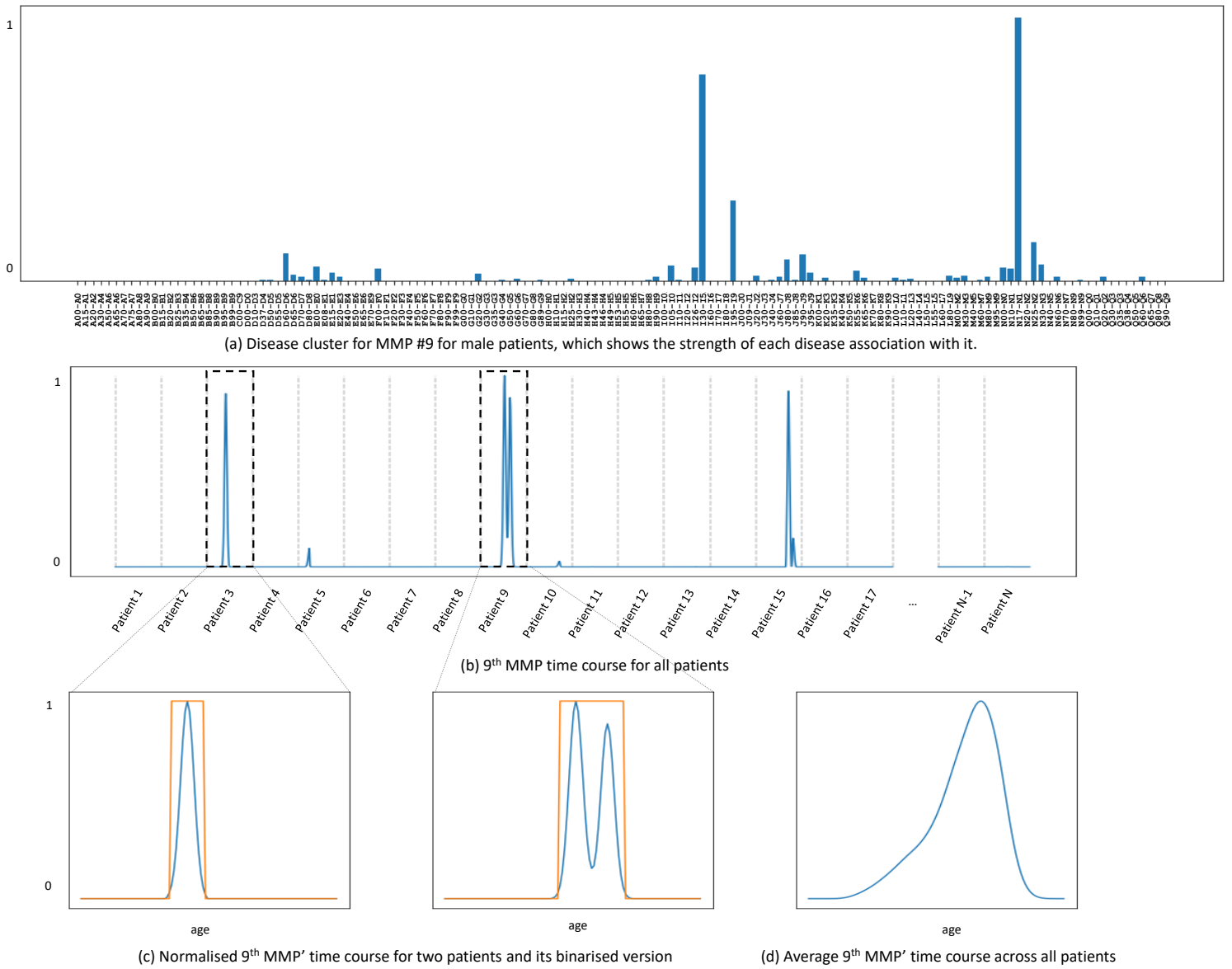


Fig. 8: Example MMP and its corresponding time courses.

(b)

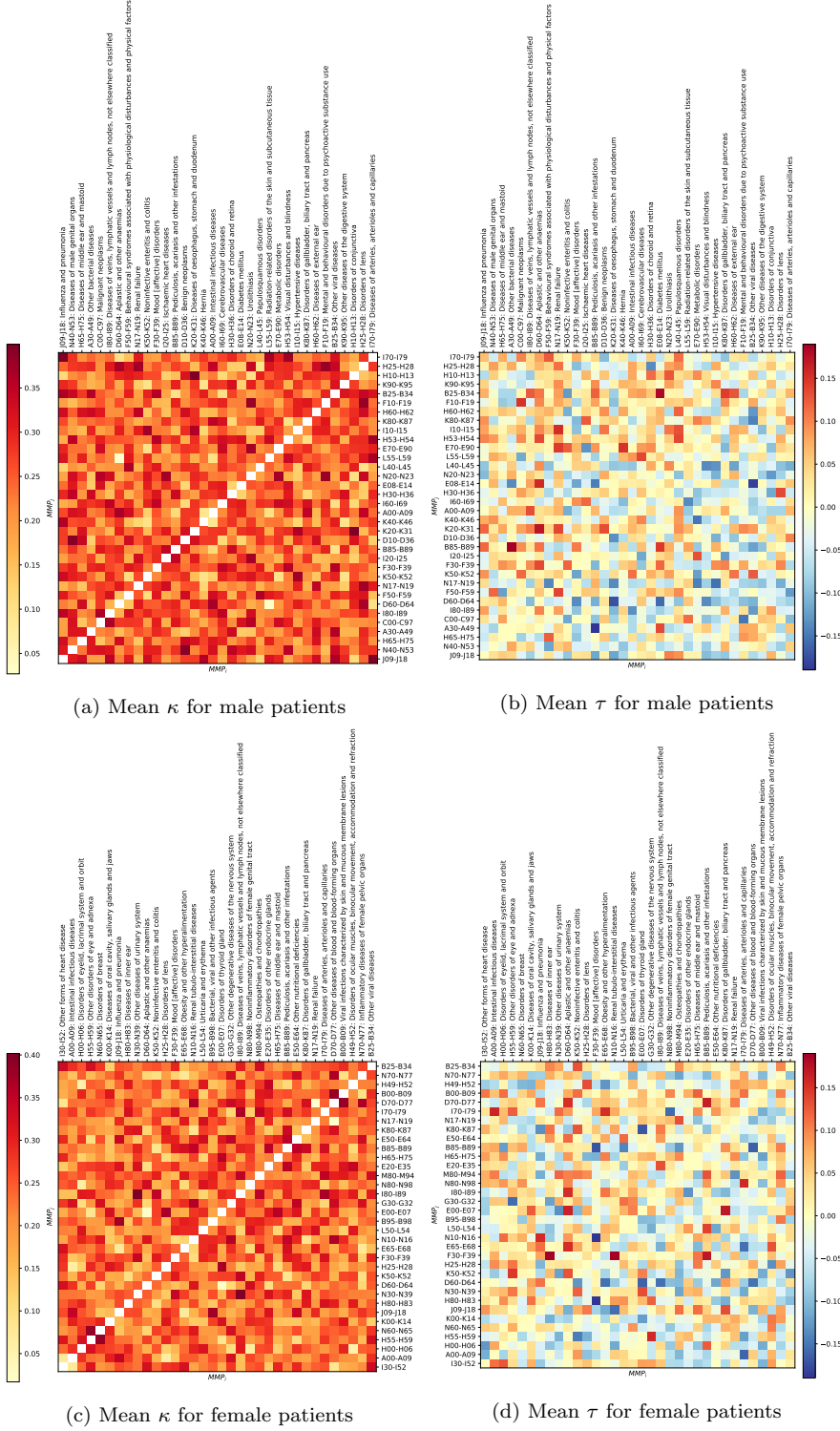


Fig. 9: Mean κ and τ for all pairs of MMP components for both male and female patients. (κ 's diagonal whitened so that other values are easy to observe). Note that κ is symmetric while τ is asymmetric.



Fig. 10: Network of MMP components for male patients. Edges are coloured with the colour of the node they originate from.



Fig. 11: Network of MMP components for female patients. Edges are coloured with the colour of the node they originate from.